Article type: Primary Research Articles

Photoperiod decelerates the advance of spring phenology of six deciduous tree species under climate warming

Running title: Photoperiod effect on spring phenology

Lin Meng[1], Yuyu Zhou[1*], Lianhong Gu[2], Andrew D. Richardson[3,4], Josep Peñuelas[5,6], Yongshuo Fu[7], Yeqiao Wang[8], Ghasserm R. Asrar[9], Hans J. De Boeck[10], Jiafu Mao[2], Yongguang Zhang[11,12,13], Zhuosen Wang[14,15]

[1]Department of Geological and Atmospheric Sciences, Iowa State University, Ames, IA, USA.
[2]Environmental Sciences Division and Climate Change Science Institute, Oak Ridge National Laboratory, Oak Ridge, TN, USA.
[3]School of Informatics, Computing and Cyber Systems, Northern Arizona University, Flagstaff, AZ, USA.
[4]Center for Ecosystem Science and Society, Northern Arizona University, Flagstaff, AZ, USA.
[5]CSIC, Global Ecology Unit CREAF-CSIC-UAB, 08913 Bellaterra, Catalonia, Spain;
[6]CREAF, 08913 Cerdanyola del Vallès, Catalonia, Spain.
[7]Beijing Key Laboratory of Urban Hydrological Cycle and Sponge City Technology, College of Water Sciences, Beijing Normal University, Beijing, China.
[8]Department of Natural Resources Science, University of Rhode Island, Kingston, RI, USA.
[9]Universities Space Research Association, Columbia, MD, USA.
[10]PLECO (Plants and Ecosystems), Department of Biology, University of Antwerp, B-2160 Wilrijk, Belgium.
[11]International Institute for Earth System Science, Nanjing University, Nanjing, China.
[12]Jiangsu Center for Collaborative Innovation in Geographical Information Resource Development and Application, Nanjing, China.
[13]Collaborative Innovation Center of Novel Software Technology and Industrialization, Nanjing, China.

[14]NASA Goddard Space Flight Center, Greenbelt, Maryland, USA.
[15]Earth System Science Interdisciplinary Center, University of Maryland, College Park, Maryland, USA.

Correspondence
Yuyu Zhou, Department of Geological and Atmospheric Sciences, Iowa State University, Ames, IA, USA, yuyuzhou@iastate.edu

Keywords: spring leaf-out, phenological model, temperature, chilling, daylength, climate change

Abstract

Vegetation phenology in spring has substantially advanced under climate warming, consequently shifting the seasonality of ecosystem process and altering biosphere-atmosphere feedbacks. However, whether and to what extent photoperiod (i.e., daylength) affects the phenological advancement is unclear, leading to large uncertainties in projecting future phenological changes. Here we examined the photoperiod effect on spring phenology at a regional scale using in situ observation of six deciduous tree species from the Pan European Phenological Network during 1980-2016. We disentangled the photoperiod effect from the temperature effect (i.e., forcing and chilling) by utilizing the unique topography of the northern Alps of Europe (i.e., varying daylength but uniform temperature distribution across latitudes) and examining phenological changes across latitudes. We found prominent photoperiod-induced shifts in spring leaf-out across latitudes (up to 1.7 days per latitudinal degree). Photoperiod regulates spring phenology by delaying early leaf-out and advancing late leaf-out caused by temperature variations. Based on these findings, we proposed two phenological models that consider the photoperiod effect through different mechanisms and compared them with a chilling model. We found that photoperiod regulation would slow down the advance in spring leaf-out under projected climate warming and thus mitigate the increasing frost risk in spring that deciduous forests will face in the future. Our findings identify photoperiod as a critical but understudied factor influencing spring phenology, suggesting that the responses of terrestrial ecosystem processes to climate warming are likely to be overestimated without adequately considering the photoperiod effect.

Introduction

Phenological stages, such as leaf-out and flowering, are sensitive to weather and climate variability, serving as indicators of integrative biological impacts of climate change (Menzel & Fabian, 1999). Finely tuned to the seasonality of the surrounding environment, phenology plays two apparently conflicting but equally important roles in minimizing the risk of damage from late frost events and maximizing the length of the growing season for carbon fixation (Basler & Körner, 2012; Larcher, 2003). Temperature directly drives the developmental rates of deciduous trees in spring but has large inter-annual variations (Peñuelas & Filella, 2001). In contrast, photoperiod (i.e., daylength) is astronomically controlled and predictable, serving as a reliable cue for seasonal progression and changing of freezing risk (Körner & Basler, 2010). Greater incidence of extreme climate events and climate warming has pushed spring phenology to new limits of inter-annual variation, exposing deciduous trees to increased risks on both ends (Richardson et al., 2018). However, it is unclear whether photoperiod would constrain the warming-induced variation of spring phenology (Basler & Körner, 2012; Way & Montgomery, 2015), leading to considerable uncertainties in the projection of phenological changes and associated land-atmosphere interactions and feedbacks (Peñuelas & Filella, 2009; Richardson et al., 2013). These uncertainties have hindered the development of effective adaptation strategies to reduce ecosystem vulnerability under the ongoing climate change (Gu et al., 2008; Hufkens et al., 2012).

Empirical evidence is inconclusive with respect to the photoperiod effect on spring phenology (Flynn & Wolkovich, 2018; Way & Montgomery, 2015; Zohner, Benito, Svenning, & Renner, 2016). Temperate and boreal forests experience dormancy in winter to withstand unfavorable environmental conditions. Environmental factors, including the degree of winter

chilling, photoperiod, and spring forcing (degree-day accumulation), trigger the dormancy release and onset of the growing season (Richardson et al., 2013). Under the same daily forcing temperature, manipulated longer photoperiod was found to advance spring phenology of late-successional species by counterbalancing the effects of lack of chilling (Caffarra & Donnelly, 2011; Laube, Sparks, Estrella, Höfler, et al., 2014). Photoperiod may also constrain the phenological development until daylength exceeds a threshold (Heide, 1993; Wareing, 1953; Zohner & Renner, 2015). In addition, the phenological variability of some species seems not to be strongly constrained by photoperiod (Richardson et al., 2018; Zohner et al., 2016). Besides the physiological variations among tree species, such divergent results could also be caused by the design of experimental manipulations, e.g., the use of seedlings or cuttings cultivated indoors as a substitute for mature trees and the use of fixed, rather than gradually extended daylength under controlled conditions (Saxe, Cannell, Johnsen, Ryan, & Vourlitis, 2001). Experimental studies are also limited to certain species and locations, leaving potentially large discrepancies across species and space in the photoperiod effect to be poorly understood.

Observational datasets that cover a wide geographic range and include abundant tree species allow for regional-scale investigations of the photoperiod effect on phenology (Vitasse & Basler, 2013). For example, the spring phenology of European beech (*Fagus sylvatica*) was found to be mainly controlled by photoperiod for southern and lower elevation populations and by temperature for northern and higher elevation populations (Wareing, 1953). Photoperiod effects are also found to be highly species-specific across European temperate zone tree species (Fu et al., 2019). However, the photoperiod effects from these studies are often challenging to interpret, given the covariation of temperature and photoperiod within a year (Flynn &

Wolkovich, 2018). As a result, the complex interactions of temperature and photoperiod on spring phenology remain unclear (Chuine, Morin, & Bugmann, 2010).

The topography of central Europe, from the Alps to northern Germany, offers a unique opportunity to disentangle the photoperiod and temperature effects on spring phenology in a natural setting. The coincidence of the increase in latitude but the decrease in elevation provides a relatively uniform temperature distribution in the background of gradual changes in daylength across latitudes. Taking advantage of this coincidence, we aim to answer the following questions: (1) Is there a photoperiod-induced latitudinal change in spring leaf-out of deciduous forests? (2) To what extent does photoperiod interact with temperature in affecting spring leaf-out? (3) How does photoperiod affect the spring leaf-out and frost risk under the projected future climate warming?

To answer these questions, we used the geographical characteristics of the study area combined with a stratification approach to maximally constrain the effects of temperature variation and isolate the effects of photoperiod on phenology. Specifically, we stratified all data into nine temperature groups and examined the latitudinal changes in spring leaf-out of six deciduous tree species in each temperature group. To test whether photoperiod causes the temperature-independent phenological changes across latitudes, we developed two photoperiod-enabled phenology models and compared them with a conventional chilling-alone model (without photoperiod effect) in predicting the changes in spring leaf-out. Finally, we examined the photoperiod effect on frost risk of the deciduous tree under future warming scenarios by projecting spring leaf-out and frost days (days from spring leaf-out to the summer solstice when daily minimum temperature < 0 °C) until 2100 using temperatures from the Coupled Model Intercomparison Project 5 (CMIP5).

Materials and Methods

Study area

Study sites of phenological observations are located in central Europe, from the Alps to northern Germany (47-55°N latitudes, Fig. 1), spanning an elevation range of 0 to 1100 m above the sea level. Elevation in this region decreases with latitude increases, resulting in similar temperatures but gradually changing daylength (Fig. 2). The long-term mean spring temperature (January 1st to April 30th) during 1980-2016 only ranges between 3.0 and 4.2 °C in 50% of the study sites (Fig. S1). Seasonal changes in daylength are larger in the north compared to in the south of the study region (Fig. S2). For example, the ranges of daylength in a given year at 55°N and 45°N are 10.2 and 6.9 hours, respectively.

Datasets

Phenological observations were collected from the Pan European Phenological Network (PEP725, http://www.pep725.eu/) (Templ et al., 2018), which is a large, long time series, and open access phenology dataset. This dataset has been widely used to investigate the effects of environmental factors on phenology. Spring leaf-out of six deciduous tree species, comprising *Aesculus hippocastanum* (Horse chestnut), *Alnus glutinosa* (Alder), *Betula pendula* (Birch), *Fagus sylvatica* (Beech), *Fraxinus excelsior* (Ash), and *Quercus robur* (Oak), was analyzed. These species have the most complete records during the study period 1980-2016, and have been used in a variety of phenology studies (Fu et al., 2019). In total, 8653 site-year-species observations at 1851 sites were used in this study. We used the phenophase leaf-out (first visible leaf stalk) in this study. We excluded records of spring leaf-out later than June 30th to reduce potential bias due to outliers.

The time series of daily mean air temperature for the study sites during the period 1980-2016 was derived from the E-OBS gridded observational dataset version 19.0 at a 0.1° spatial resolution (Cornes, van der Schrier, van den Besselaar, & Jones, 2018). The temperature was used to calculate forcing and chilling accumulations, mean temperature during winter and spring, and to run phenological models.

Future daily minimum and mean temperatures during the period 2006-2100 for the study area were derived from the CMIP5 (https://cds.climate.copernicus.eu/cdsapp#!/) for the experiment of Representative Concentration Pathway 8.5 (RCP 8.5) scenario from the model of Community Climate System Model (CCSM) 4.0 of U.S. National Center for Atmospheric Research (NCAR). We used the experiment of RCP 8.5 to show the largest possible phenological changes under projected future climate warming. We calculated the regional mean time series of daily mean and minimum temperatures. The daily minimum temperature was then used to calculate frost days and the daily mean temperature was used to run phenological models.

We used a 90 m digital elevation dataset (http://srtm.csi.cgiar.org) that provides continuous topography surfaces (Jarvis, 2008) from NASA's Shuttle Radar Topography Mission (SRTM).

Daylength was calculated as a function of latitude (L) and day of the year (DOY) using equation (1) (Forsythe, Rykiel Jr, Stahl, Wu, & Schoolfield, 1995):

$$D = 24 - \frac{24}{\pi} \times cos^{-1}\left(\frac{sin\frac{0.8333\pi}{180} + sin\frac{\pi}{180}sin\varphi}{cos\frac{L\pi}{180} \times cos\varphi}\right) \quad (1)$$

$$\varphi = \sin^{-1}(0.29795 \times \cos\theta) \quad (2)$$

$$\theta = 0.2163108 + 2\tan^{-1}(0.9671396 \times \tan(0.0086 \times (DOY\text{-}186))) \quad (3)$$

where D is daylength, φ is the sun's declination angle, θ is revolution angle; φ and θ are measured in radians.

172 **Experimental design**

173 To minimize the temperature effect on spring leaf-out across latitudes, we stratified the
174 data into nine temperature groups based on three forcing and three chilling accumulations at
175 high, medium, and low levels for each deciduous tree species. Forcing accumulation was defined
176 as an integration of daily mean temperature above a temperature threshold (5 °C) throughout the
177 preseason (from November 1st in the preceding year to leaf-out) (Fu et al., 2015). Chilling
178 accumulation was defined as the number of days when the daily mean temperature was below
179 5 °C (Kramer, 1994). First, we divided all data into three forcing levels using 33.3% and 66.6%
180 quantiles of all forcing accumulations during the period 1980-2016. Then, within each forcing
181 level, we further divided data into three chilling levels using 33.3% and 66.6% quantiles of all
182 chilling accumulations of that forcing level during the period 1980-2016. We analyzed changes
183 in spring leaf-out across latitudes in each temperature group. This stratification approach also
184 enables us to investigate the interaction between photoperiod and temperature by comparing the
185 magnitude of latitudinal leaf-out changes across temperature groups.

186 To evaluate phenological models in terms of predicting the latitudinal trend of spring
187 leaf-out, we ran models and compared model performance using data from the 65-75% quantiles
188 of forcing accumulations and 25-35% quantiles of chilling accumulations. These criteria were
189 used because we found the delay trends of spring leaf-out across latitudes were the most
190 pronounced in high forcing and low chilling groups. We also examined the latitudinal trends in
191 forcing and chilling to test whether there are effects of forcing and chilling on the latitudinal
192 trends in spring leaf-out. We further conducted two sensitivity analyses using a wider band (60-
193 80% quantiles of forcing accumulations and 20-40% quantiles of chilling accumulations) and a

narrower band (70-75% quantiles of forcing accumulations and 25-30% quantiles of chilling accumulations) to test the effect of samples size on results.

Frost risk was represented by the number of frost days during the first half of the growing season, i.e., from spring leaf-out to the summer solstice on June 22nd. Frost days were calculated as days when the daily minimum temperature was below 0 °C (Liu et al., 2018). To quantify the role of photoperiod in mitigating frost risks, we compared the spring leaf-out and total frost days using daily minimum temperatures from CMIP5 during the period 2007-2100 predicted by three phenological models.

Phenological models

We proposed two photoperiod-enabled models, comprising a photo-threshold model and a photo-chilling model, which incorporated the photoperiod effect in predicting spring leaf-out. The photo-threshold model includes photoperiod and forcing processes while the photo-chilling model includes photoperiod (but different from the photo-threshold model), chilling, and forcing processes. Specifically, the photo-threshold model assumes the forcing process starts when the daylength is above a minimum threshold; spring leaf-out is predicted to occur when (1) forcing accumulation reaches its threshold or (2) daylength is above a maximum threshold (Melaas, Friedl, & Richardson, 2016). The photo-threshold model was developed from the growing-degree-day model that only considers the forcing process, which used an arbitrary date (e.g., January 1st) as the start date for the forcing accumulation. We replaced the arbitrary date with a minimum daylength threshold to account for the spatial variation of the start of the forcing process. We also added a maximum daylength threshold as the latest end date of the forcing process to ensure spring leaf-out could be triggered in the case when forcing cannot reach its requirement in extreme cold years. The photo-chilling model assumes trees accumulate forcing

and chilling starting from winter, and spring leaf-out is predicted to occur when forcing accumulation reaches a threshold (determined by chilling accumulation). The effectiveness of forcing accumulation is affected by photoperiod, which is chilling-dependent (i.e., strong photoperiod effect under low chilling)(Caffarra, Donnelly, Chuine, & Jones, 2011). The photo-chilling model was developed from a widely used chilling model, i.e., parallel model, which considers the forcing and chilling processes (Hänninen, 1990), and we added a chilling-dependent photoperiod variable to this model to adjust the efficiency of forcing accumulation. We also include the original parallel chilling model as a representation of a modeling scheme without consideration of the photoperiod effect and hereafter termed it as chilling-alone model.

We calibrated models using 80% of observations (i.e., data during the period 1980-2010 across all sites) for each deciduous tree species, respectively. The objective function of the calibration process was the minimum root-mean-square error (RMSE) between prediction and observation. The calibrated parameters are shown in Table 1. We evaluated models using the remaining 20% of observations (i.e., data during the period 2011-2016 across all sites) for each deciduous tree species, and then applied three models to predict spring leaf-out and its latitudinal trends. We further compared the model performance in simulating the historical interannual variation in phenology in terms of RMSE for each species. We also used the models to project future changes in spring leaf-out using projected daily average temperatures from CMIP5 for the period 2007-2100. We then used the predicted spring leaf-out to calculate frost days.

The phenological models are shown below.

Photo-threshold model

$$R_f(t) = \begin{cases} x(t) - T_{\text{base}} & x(t) > T_{\text{base}} \\ 0 & x(t) \le T_{\text{base}} \end{cases}$$

$$S_f(t) = \sum_{t_0} R_f(x(t))$$

Spring leaf-out is predicted to occur when $S_f(t) \geq F^*$ or $DL(t) \geq DL_{end}^*$. The forcing process starts at t_0, that is when $DL(t) \geq DL_{start}^*$. t is day of year, $x(t)$ is daily temperature, $DL(t)$ is daily daylength, DL_{start}^* is the minimum daylength threshold to trigger the forcing process, DL_{end}^* is the maximum daylength threshold, F^* is the forcing requirement, $R_f(t)$ is the rate of forcing. $S_f(t)$ is the state of forcing, calculated as the summation of $R_f(t)$ from DL_{start}^* to the predicted spring leaf-out. T_{base} is base temperature (5 °C). DL_{start}^*, DL_{end}^*, and F^* are parameters to be calibrated.

Photo-chilling model

$$R_f(t) = \begin{cases} \dfrac{28.4}{1 + \exp\,(3.4 - 0.185 * x(t))} & x(t) > T_{\text{base}} \\ 0 & x(t) \leq T_{\text{base}} \end{cases}$$

$$S_f(t) = \sum_{t_0} R_f(x(t)) \times R_p$$

$$R_c(t) = \begin{cases} 0 & x(t) \geq 10.4 \text{ or } x(t) \leq -3.4 \\ \dfrac{x(t) + 3.4}{T_{\text{opt}} + 3.4} & -3.4 < x(t) \leq T_{\text{opt}} \\ \dfrac{x(t) - 10.4}{T_{\text{opt}} - 10.4} & T_{\text{opt}} < x(t) < 10.4 \end{cases}$$

$$S_c(t) = \sum_{t_0} R_c(x(t))$$

$$R_p(t) = \frac{DL(t)}{12} \times e^{c \times S_c(t)}$$

Spring leaf-out is predicted to occur when $S_f(t) \geq a * \exp\,(b * S_c(t))$, where $b < 0$. t is the day of year, $x(t)$ is daily temperature, $DL(t)$ is daily daylength, T_{opt} is the optimum temperature for chilling accumulation, $S_f(t)$ and $S_c(t)$ are the states of forcing and chilling, respectively. $R_f(t)$,

$R_c(t)$, and $R_p(t)$ are the rates of forcing, chilling, and photoperiod, respectively. Forcing and chilling accumulations start at t_0, i.e., November 1st in the preceding year in this study. T_{base} is base temperature (5 °C). *a, b, c*, and T_{opt} are parameters to be calibrated.

Chilling-alone model

$$R_f(t) = \begin{cases} \dfrac{28.4}{1 + \exp\,(3.4 - 0.185 * x(t))} & x(t) > T_{\text{base}} \\ 0 & x(t) \le T_{\text{base}} \end{cases}$$

$$S_f(t) = \sum_{t_0} R_f(x(t))$$

$$R_c(t) = \begin{cases} 0 & x(t) \ge 10.4 \text{ or } x(t) \le -3.4 \\ \dfrac{x(t) + 3.4}{T_{\text{opt}} + 3.4} & -3.4 < x(t) \le T_{\text{opt}} \\ \dfrac{x(t) - 10.4}{T_{\text{opt}} - 10.4} & T_{\text{opt}} < x(t) < 10.4 \end{cases}$$

$$S_c(t) = \sum_{t_0} R_c(x(t))$$

Spring leaf-out is predicted to occur when $S_f(t) \ge a * \exp\,(b * S_c(t))$, where b < 0. This model shares the same parameters with the photo-chilling model but without the photoperiod variable.

Results

Photoperiod-induced shifts in spring leaf-out

We found significant latitudinal shifts in spring leaf-out ($P < 0.05$) in 49 of the 54 temperature-species groups (i.e., 9 temperature × 6 species groups, Table 2). Among these 49 groups, spring leaf-out delayed with increasing latitude in 44 groups (i.e., earlier spring leaf-out in the southern region), as indicated by positive slopes (day $^{o}L^{-1}$, i.e., number of days delayed in

spring leaf-out per latitudinal degree increase, $P < 0.05$). The greatest delays occurred in the medium forcing and low chilling groups, i.e., spring leaf-out delayed > 1.2 day $^{o}L^{-1}$ across the six deciduous tree species (largest delay in *Q. robur*: 1.7 day $^{o}L^{-1}$, $P < 0.05$, Fig. 3 and Table 2). In contrast, spring leaf-out advanced, up to -0.3 day $^{o}L^{-1}$, in the high forcing and high chilling groups of *A. hippocastanum*, *A. glutinosa*, *F. excelsior*, *Q. robur*, and in the low forcing and high chilling group for *B. pendula* ($P < 0.05$, Figs. S3-S4 and Table 2). The degree of latitudinal changes was very different among species, ranging from 0.8 ± 0.6 day $^{o}L^{-1}$ (mean ± standard deviation, *Q. robur*) to 0.5 ± 0.5 day $^{o}L^{-1}$ (*A. glutinosa*) across all temperature groups (Table 2).

Modeling results directly supported that the photoperiod effect is the main contributor to the temperature-independent latitudinal shifts in spring leaf-out. All three models captured the historical interannual variation of spring leaf-out (Fig. S5 and Table S1). Both photoperiod-enabled models showed improvements in predicting spring leaf-out for all six deciduous tree species in terms of root mean square error (RMSE, photo-threshold: 8.3 ± 1.1 days; photo-chilling: 8.3 ± 0.9 days) and correlation (photo-threshold: 0.62 ± 0.07; photo-chilling: 0.60 ± 0.06), compared to the chilling-alone model (RMSE: 9.7 ± 0.8 days; correlation: 0.55 ± 0.07) (Fig. 4). More importantly, both photoperiod-enabled models reproduced the observed latitudinal delay in spring leaf-out (i.e., positive slopes) for all six deciduous tree species ($P < 0.01$, Fig. 5, see Discussion), although the photo-chilling model underestimated and the photo-threshold model overestimated the magnitude of the latitudinal delay for most species. In contrast, the chilling-alone model only reproduced 30% (0.39 day $^{o}L^{-1}$) and 32% (0.33 day $^{o}L^{-1}$) of magnitudes of the latitudinal delay for *F. excelsior* and *Q. robur* ($P < 0.01$), respectively, and predicted no trends for the rest four species (Fig. 5). The differences in slope between the photo-chilling and chilling-alone models (Fig. 5) indicate the photoperiod effect, since these two

297 models are the same except that the former considers the photoperiod effect. The chilling-alone
298 model predicted no trends in spring leaf-out across latitudes, which was expected because the
299 chilling-alone model depends solely on forcing and chilling and neither of them showed a trend
300 across latitudes (Table S2). Such homogenous distribution of forcing and chilling further
301 supports that the latitudinal shifts in spring leaf-out were not caused by a temperature effect.

302 **The underlying mechanism of the photoperiod effect**

303 The photo-threshold model well captured the observed spatial variation in spring leaf-out
304 for the six deciduous tree species (e.g., later leaf-out at higher latitudes, depicted by the gray
305 curve in Fig. 6), but neither the photo-chilling model nor the chilling-alone model did the same
306 (Fig. 6). Such contrast in model performances indicates that photoperiod affects the spatial
307 variation in spring leaf-out mainly by imposing a threshold to trigger the forcing process, rather
308 than varying with chilling conditions to influence the effectiveness of forcing accumulation. The
309 photo-chilling and chilling-alone models predicted a similar latitudinal distribution pattern
310 (depicted by the gray curve), but the former showed a considerably improved prediction of
311 latitudinal trends of spring leaf-out (Fig. 6c-d) by simply adding photoperiod as an additional
312 variable. We obtained similar results using either a wider or a narrower forcing and chilling
313 threshold to select data (Figs. S6-S7), indicating that the general patterns are robust for different
314 selection criteria and sample sizes. These results illustrate that incorporating the photoperiod
315 effect into phenological models greatly improves the predictability of spring leaf-out and its
316 spatial variation.

317 In addition, model performance in predicting latitudinal delay in spring leaf-out varied
318 greatly across species, indicating a highly species-specific phenological dependence on the
319 photoperiod effect. Specifically, the photo-chilling model best predicted the magnitude of delay

for *A. hippocastanum, A. glutinosa, B. pendula*, and *F. sylvatica,* while the photo-threshold model best predicted the magnitude of delay for *F. excelsior* and *Q. robur* (Fig. 5). The photo-threshold model overestimated the magnitudes, especially for *A. hippocastanum*, *A. glutinosa*, and *B. pendula*, whereas the photo-chilling model underestimated the magnitudes of delay for four out of six species (ranging from 65% for *F. excelsior* to 86% for *A. hippocastanum*, Figs. 5 and 6).

Interactions between photoperiod and temperature

The photoperiod effect on spring leaf-out showed clear interactions with temperature (Fig. 7). How and to what extent photoperiod changed spring leaf-out across latitudes depended on temperature, as represented by the nine forcing and chilling accumulation groups. As shown in Fig. 7, spring leaf-out either remained unchanged or significantly advanced across latitudes (negative slopes) in the high forcing and high chilling group (i.e., the upper right portion of the data point, e.g., *F. sylvatica* showed the largest advance at -0.3 day $^{o}L^{-1}$), while leaf-out mostly showed significant delay northwards in other temperature groups (positive slopes, earlier leaf-out in the southern region) ($P < 0.05$). There were greater delays in low chilling group (i.e., the left portion of the data point in Fig. 7, 1.1 ± 0.4 day $^{o}L^{-1}$, mean ± standard deviation of slopes across six deciduous tree species and forcing groups) than in the medium chilling group (0.7 ± 0.3 day $^{o}L^{-1}$), and the delay effect gradually diminished or became non-significant towards high chilling and low forcing groups (i.e., the bottom right portion in Fig. 7, 0.1 ± 0.2 day $^{o}L^{-1}$). When putting together the changes in photoperiod effect with spring leaf-out, we found the advancing effect of photoperiod (negative slopes, Fig. 7) occurred when spring leaf-out was relatively late (i.e., brown in the upper right portion in Fig. 7 subfigures) while the delaying effect existed for the

342 mid-to early spring leaf-out (gray and green in Fig. 7 subfigures). The results are relatively
343 consistent across all six deciduous tree species despite differences in magnitude.

344 **Mitigation of frost risks**

345 All three models show that spring leaf-out will be significantly advanced under climate
346 warming ($P < 0.001$, Fig. 8). More importantly, models show that photoperiod slows down the
347 advancement of spring leaf-out and reduces the frost risk of deciduous trees under the projected
348 warming climate. The advancing rate of spring leaf-out predicted by the chilling-alone model (-
349 4.12 ~ -3.15 day decade^{-1}) was around twice what was predicted by two photoperiod-enabled
350 models (-2.00 ~ -1.61 day decade^{-1}) ($P < 0.001$, Table 3). According to the chilling-alone model,
351 spring leaf-out was predicted to advance up to 36 days by 2100, in contrast to only 17 days
352 predicted by the two photoperiod-enabled models across six deciduous species (Fig. 8).
353 Consequently, the chilling-alone model (mean ± standard deviation: 22 ± 11 days) predicts 21
354 more accumulated frost days than the photoperiod-enabled models (mean ± standard deviation: 1
355 ± 0.5 days) for the six deciduous tree species from 2007 to 2100 (Fig. 8), demonstrating the
356 effective mitigation of frost risk by photoperiod. The spring leaf-out of *F. sylvatica, F. excelsior,*
357 and *Q. robur* showed less advance by 2100, compared to that of *A. hippocastanum, A. glutinosa,*
358 and *B. pendula* (Table 3). In addition, the accumulated frost days for *F. sylvatica, F. excelsior,*
359 and *Q. robur* were significantly fewer compared to those for *A. hippocastanum, A. glutinosa,* and
360 *B. pendula*, indicating highly species-specific risk of frost damage, with higher risks for earlier
361 phenology species.

362

363 **Discussion**

364 The photoperiod effect on phenology we reported here is a two-way effect, i.e.,
365 advancing excessive late spring leaf-out and delaying excessive early spring leaf-out caused by
366 temperature variation. The advance and delay effects of photoperiod have been proposed and
367 discussed conceptually in previous studies (Basler & Körner, 2014; Vitasse & Basler, 2013; Way
368 & Montgomery, 2015), and the delay effect has been reported from experimental studies (Zohner
369 & Renner, 2015). However, this is the first study to reveal photoperiod advances excessive late
370 spring leaf-out at the regional scale based on field observational datasets. Our finding points to
371 the necessity of considering photoperiod together with temperature in predicting phenological
372 changes under climate warming. Previously, it has been often assumed that temperature has a
373 prominent effect on spring phenology at the current climate regime; as a result, the photoperiod
374 effect and its interaction with temperature have not been as widely studied as the temperature
375 effect itself (Basler & Körner, 2014; Meng, Mao, et al., 2020; Tang et al., 2016). As the
376 scientific communities focus on the considerable advancement of spring phenology driven by
377 climate warming, our study calls attention to that photoperiod actually mitigates and may
378 eventually limit such advancement in the future. As the warming trend continues, the
379 temperature effect on phenology may decline whereas photoperiodic cues may become
380 increasingly critical to spring phenology. Our findings also have significant implications for
381 forecasting forest vulnerability in a warming world. Although extreme climate events may lead
382 to increased risks of spring leaf-out (Gu et al., 2008), photoperiod may reduce the risk of frost
383 damage associated with premature onset of tree growth by decelerating the advance in spring
384 phenology.

385 This study addressed the challenge to disentangle the photoperiod and temperature effects
386 on spring leaf-out by using the natural topography of the Alps, i.e., spatially relatively

387 homogenous temperatures caused by higher elevations at lower latitudes and a significant
388 latitudinal gradient of daylength. We further constrained temperature variation to the minimum
389 by dividing all site-year data into nine temperature groups according to forcing and chilling
390 accumulation. Although there was possibly still minor temperature variation within each group,
391 the trend of spring leaf-out in Fig. 3 was mainly caused by photoperiod, not temperature, for two
392 reasons. First, the photo-chilling model simulated the latitudinal trend of leaf-out, but the
393 chilling-alone model did not (Figs. 5-6). Having the same model structure, these two models
394 only differ in whether considering photoperiod effect. Therefore, photoperiod mainly caused the
395 difference in simulated spring leaf-out between these two models, i.e., the latitudinal trend of
396 spring leaf-out. Second, we used observational data within a very narrow temperature range (i.e.,
397 65%-75% quantiles of forcing and 25%-35% quantiles of chilling) without latitudinal trend of
398 forcing and chilling (Table S2), and we still see the same magnitude in the latitudinal trend of
399 spring leaf-out (Fig. 6a), as compared to in the 33% quantile group in Fig. 3. This indicates
400 temperature variation is not the main reason for the observed leaf-out trend.
401 The two photoperiod-enabled models proposed in our study are advantageous to
402 correlative analyses between spring leaf-out and photoperiod to disentangle the photoperiod
403 effect and understand the underlying mechanisms. This is because a photoperiod model describes
404 the photoperiod effect as a complete and continuous process over a period, while the correlative
405 analyses only depict the photoperiod effect of a single date. The biases resulted from this single
406 date approach are particularly pronounced if the study areas extend over wide latitudinal ranges,
407 due to the distinct seasonal changes in daylength across latitudes (e.g., relatively longer
408 daylength occurs before the spring equinox at lower latitudes and after the spring equinox at
409 higher latitudes, Fig. S2). In contrast, our models precisely account for the reversing of relative

daylength before and after the spring equinox across latitudes. A photoperiod model also allows hypothesis testing on the underlying mechanisms of the photoperiod effect and predicting phenological changes under contrasting future scenarios so that the photoperiod effect on frost risk mitigation can be quantified.

Both the photo-threshold and photo-chilling models reproduced the observed patterns in spring leaf-out, but they represent contrasting underlying mechanisms of photoperiod effects (Basler & Körner, 2014; Caffarra & Donnelly, 2011; Vitasse & Basler, 2013; Vitasse, Signarbieux, & Fu, 2018). In the photo-threshold model, the observed delay and advance effects of photoperiod are represented by the minimum and maximum daylength thresholds, respectively. Specifically, trees in the south of this study area reach the minimum threshold and start the forcing process earlier than trees in the north (Fig. S2), resulting in an earlier spring leaf-out in the south (i.e., delay effect). In an extremely cold year when the forcing threshold cannot be reached, trees in the north reach the maximum threshold earlier than trees in the south (Fig. S2), leading to an earlier spring leaf-out at higher latitudes (i.e., advance effect). In addition, the photo-threshold model assumes that the daylength does not affect phenology before the minimum threshold is reached, which is consistent with the findings from experimental studies (Zohner & Renner, 2015). In terms of the photo-chilling model, longer daylength in the south before the spring equinox contributes to a stronger photoperiod effect, which causes faster forcing accumulations and leads to an earlier spring leaf-out. On the contrary, in extreme cold years, the efficiency of forcing accumulation gradually increases as the photoperiod lengthens through spring (especially prominent at higher latitudes, e.g., 55°N in Fig. S2), mitigating late spring leaf-out and causing the advancing trend across latitudes.

In general, photo-threshold and photo-chilling models show similar performance, indicating that despite the photo-chilling model has an additional chilling process than the photo-threshold model, including such a process does not always lead to the improved prediction for all species in our study area. For instance, the photo-chilling model shows better prediction on the latitudinal trend of spring leaf-out for four out of six species (e.g., *A. hippocastanum, A. glutinosa, B. pendula, F. sylvatica*, Fig. 5) than the photo-threshold model. Moreover, previous studies also showed the model complexity did not necessarily lead to improved accuracy, partly because not all species require chilling explore (Hänninen et al., 2019). For example, Basler et al. (2016) reported simple models (e.g., models only consider forcing process) showed similar performance to more complex models such as chilling-alone models in six temperate tree species across central Europe. The two photoperiod-enabled models serve as examples to incorporate photoperiod to improve phenology prediction, but they are not the only model structures and do not exclude other possible representations of the photoperiod effect in phenological models.

The underlying mechanisms and/or the strength of the photoperiod effect are highly species-specific. Such a species variation may be linked to the inherently different tolerant levels to the trade-off between late-season frost risk and productivity evolved in species' life history (Borchert, Robertson, Schwartz, & Williams-Linera, 2005; Hänninen et al., 2019; Vitasse & Basler, 2013), that is, opportunistic and freezing-resistant species are more temperature-dependent and 'risky' while late-successional species are more photoperiod sensitive and 'conservative' to follow temperature variation (Basler & Körner, 2012). The photoperiod effect may also vary among populations within one species (Vitasse & Basler, 2013), which is not considered in this study. The sensitivity of the photoperiod effect may interact with other factors such as nutrition; trees with abundant nutrition tend to follow a more risky strategy to maximize

455 growing season length probably due to higher concentrations of proteins that resist the formation
456 of icicles (Tateno & Takeda, 2003). These different photoperiod sensitivities may potentially
457 lead to more divergent frost risks that different species will experience under climate warming
458 (Basler & Körner, 2012). Plant-community structures and geographical distribution of species
459 may even be changed in the long run due to the unevenly increased risks.

460 Adaptation or acclimation of trees to environments under climate change has been
461 reported and discussed (Bennie, Kubin, Wiltshire, Huntley, & Baxter, 2010). However, the
462 capacity of deciduous trees to genetically or physiologically adapt to warmer conditions in terms
463 of the timing of growth is unclear. Understanding the degree of adaptation of deciduous trees to
464 photoperiod effect across the wide range of latitudes will enable further advances in phenological
465 modeling. Experimental studies on manipulating temperature and daylength are needed to
466 ascertain the photoperiod mechanisms controlling phenology, so that more credible model
467 extrapolations can be undertaken. In addition, extending the findings of this regional study to the
468 global scale would require consideration of interactions with other environmental factors, such as
469 precipitation, soil moisture, and diurnal temperature range (Laube, Sparks, Estrella, & Menzel,
470 2014; Meng, Zhou, et al., 2020). Besides climate conditions, physical and chemical properties of
471 soil such as the concentration of exchangeable soil potassium and soil acidity are also shown to
472 have a significant impact on spring phenology at the scale of small forest watersheds (Lapenis et
473 al., 2017).

474 This study provides observational and model-based evidence that photoperiod decelerates
475 the advance in spring phenology and thus reduces the frost risks under climate warming. The
476 delay effect of photoperiod limits the risk of damage from late frost events, while the advance
477 effect allows trees to take full advantage of the growing season for carbon fixation. The advance

effect suggests that the underlying mechanisms on photoperiod-temperature interaction may be more complex than the notion that photoperiod may substitute chilling requirements as previously reported (Caffarra & Donnelly, 2011; Laube, Sparks, Estrella, Höfler, et al., 2014). As warmer climate pushes spring phenology to the edge of the interannual variation especially the early edge, the delay effect of photoperiod will become more prominent while the advance effect will be reduced. Our results reconcile contradictory hypotheses about the interaction between photoperiod and temperature in regulating spring leaf-out (Flynn & Wolkovich, 2018; Way & Montgomery, 2015; Zohner et al., 2016). Current Earth system models need to accurately incorporate the photoperiod effect on spring phenology, since it may substantially change the trajectory of the land feedbacks to the Earth system under future warming. Increased understanding of the photoperiod effect on phenology is also crucial to ascertain whether climate warming will increase the risk of spring frost damage to terrestrial ecosystems (Ault et al., 2013; Gu et al., 2008).

References

Ault, T., Henebry, G., De Beurs, K., Schwartz, M., Betancourt, J. L., & Moore, D. (2013). The false spring of 2012, earliest in North American record. *Eos, Transactions American Geophysical Union, 94*(20), 181-182.

Basler, D. (2016). Evaluating phenological models for the prediction of leaf-out dates in six temperate tree species across central Europe. *Agricultural and Forest Meteorology, 217*, 10-21.

Basler, D., & Körner, C. (2012). Photoperiod sensitivity of bud burst in 14 temperate forest tree species. *Agricultural and Forest Meteorology, 165*, 73-81.

Basler, D., & Körner, C. (2014). Photoperiod and temperature responses of bud swelling and bud burst in four temperate forest tree species. *Tree physiology, 34*(4), 377-388.

Bennie, J., Kubin, E., Wiltshire, A., Huntley, B., & Baxter, R. (2010). Predicting spatial and temporal patterns of bud‐burst and spring frost risk in north‐west Europe: the implications of local adaptation to climate. *Global Change Biology, 16*(5), 1503-1514.

Borchert, R., Robertson, K., Schwartz, M. D., & Williams-Linera, G. (2005). Phenology of temperate trees in tropical climates. *International Journal of Biometeorology, 50*(1), 57-65.

Caffarra, A., & Donnelly, A. (2011). The ecological significance of phenology in four different tree species: effects of light and temperature on bud burst. *International Journal of Biometeorology, 55*(5), 711-721.

Caffarra, A., Donnelly, A., Chuine, I., & Jones, M. B. (2011). Modelling the timing of Betula pubescens budburst. I. Temperature and photoperiod: a conceptual model. *Climate Research, 46*(2), 147-157.

Chuine, I., Morin, X., & Bugmann, H. (2010). Warming, photoperiods, and tree phenology. *Science, 329*(5989), 277-278.

Cornes, R. C., van der Schrier, G., van den Besselaar, E. J., & Jones, P. D. (2018). An ensemble version of the E‐OBS temperature and precipitation data sets. *Journal of Geophysical Research: Atmospheres, 123*(17), 9391-9409.

Flynn, D., & Wolkovich, E. (2018). Temperature and photoperiod drive spring phenology across all species in a temperate forest community. *New Phytologist, 219*(4), 1353-1362.

Forsythe, W. C., Rykiel Jr, E. J., Stahl, R. S., Wu, H.-i., & Schoolfield, R. M. (1995). A model comparison for daylength as a function of latitude and day of year. *Ecological Modelling, 80*(1), 87-95.

Fu, Y. H., Piao, S., Vitasse, Y., Zhao, H., De Boeck, H. J., Liu, Q., . . . Janssens, I. A. (2015). Increased heat requirement for leaf flushing in temperate woody species over 1980–2012: effects of chilling, precipitation and insolation. *Global Change Biology, 21*(7), 2687-2697.

Fu, Y. H., Zhang, X., Piao, S., Hao, F., Geng, X., Vitasse, Y., . . . Janssens, I. A. (2019). Daylength helps temperate deciduous trees to leaf‐out at the optimal time. *Global Change Biology*, 25.7: 2410-2418.

Gu, L., Hanson, P. J., Post, W. M., Kaiser, D. P., Yang, B., Nemani, R., . . . Meyers, T. (2008). The 2007 eastern US spring freeze: increased cold damage in a warming world? *BioScience, 58*(3), 253-262.

Hänninen, H. (1990). Modelling bud dormancy release in trees from cool and temperate regions.

Hänninen, H., Kramer, K., Tanino, K., Zhang, R., Wu, J., & Fu, Y. H. (2019). Experiments Are Necessary in Process-Based Tree Phenology Modelling. *Trends in plant science, 24*(3), 199-209.

Heide, O. (1993). Dormancy release in beech buds (Fagus sylvatica) requires both chilling and long days. *Physiologia Plantarum, 89*(1), 187-191.

Hufkens, K., Friedl, M. A., Keenan, T. F., Sonnentag, O., Bailey, A., O'Keefe, J., & Richardson, A. D. (2012). Ecological impacts of a widespread frost event following early spring leaf ‐ out. *Global Change Biology, 18*(7), 2365-2377.

Jarvis, A. (2008). Hole-field seamless SRTM data, International Centre for Tropical Agriculture (CIAT). *http://srtm. csi. cgiar. org*.

Körner, C., & Basler, D. (2010). Response—Warming, Photoperiods, and Tree Phenology. *Science, 329*(5989), 278-278.

Kramer, K. (1994). Selecting a model to predict the onset of growth of Fagus sylvatica. *Journal of Applied Ecology*, 172-181.

Lapenis, A. G., Lawrence, G. B., Buyantuev, A., Jiang, S., Sullivan, T. J., McDonnell, T. C., & Bailey, S. (2017). A Newly Identified Role of the Deciduous Forest Floor in the Timing of Green ‐ Up. *Journal of Geophysical Research: Biogeosciences, 122*(11), 2876-2891.

Larcher, W. (2003). *Physiological plant ecology: ecophysiology and stress physiology of functional groups*: Springer Science & Business Media.

Laube, J., Sparks, T. H., Estrella, N., Höfler, J., Ankerst, D. P., & Menzel, A. (2014). Chilling outweighs photoperiod in preventing precocious spring development. *Global Change Biology, 20*(1), 170-182.

Laube, J., Sparks, T. H., Estrella, N., & Menzel, A. (2014). Does humidity trigger tree phenology? Proposal for an air humidity based framework for bud development in spring. *New Phytologist, 202*(2), 350-355.

Liu, Q., Piao, S., Janssens, I. A., Fu, Y., Peng, S., Lian, X., . . . Wang, T. (2018). Extension of the growing season increases vegetation exposure to frost. *Nature Communications, 9*(1), 426.

Melaas, E. K., Friedl, M. A., & Richardson, A. D. (2016). Multiscale modeling of spring phenology across Deciduous Forests in the Eastern United States. *Global Change Biology, 22*(2), 792-805.

Meng, L., Mao, J., Zhou, Y., Richardson, A. D., Lee, X., Thornton, P. E., . . . Shi, X. (2020). Urban warming advances spring phenology but reduces the response of phenology to temperature in the conterminous United States. *Proceedings of the National Academy of Sciences, 117*(8), 4228-4233.

Meng, L., Zhou, Y., Li, X., Asrar, G. R., Mao, J., Wanamaker Jr, A. D., & Wang, Y. (2020). Divergent responses of spring phenology to daytime and nighttime warming. *Agricultural and Forest Meteorology, 281*, 107832.

Menzel, A., & Fabian, P. (1999). Growing season extended in Europe. *Nature, 397*(6721), 659-659.

Peñuelas, J., & Filella, I. (2001). Responses to a warming world. *Science, 294*(5543), 793-795.

Peñuelas, J., & Filella, I. (2009). Phenology feedbacks on climate change. *Science, 324*(5929), 887-888.

Richardson, A. D., Hufkens, K., Milliman, T., Aubrecht, D. M., Furze, M. E., Seyednasrollah, B., . . . Heiderman, R. R. (2018). Ecosystem warming extends vegetation activity but heightens vulnerability to cold temperatures. *Nature*, 1.

582 Richardson, A. D., Keenan, T. F., Migliavacca, M., Ryu, Y., Sonnentag, O., & Toomey, M.
583 (2013). Climate change, phenology, and phenological control of vegetation feedbacks to
584 the climate system. *Agricultural and Forest Meteorology, 169*, 156-173.
585 Saxe, H., Cannell, M. G., Johnsen, Ø., Ryan, M. G., & Vourlitis, G. (2001). Tree and forest
586 functioning in response to global warming. *New Phytologist, 149*(3), 369-399.
587 Tang, J., Körner, C., Muraoka, H., Piao, S., Shen, M., Thackeray, S. J., & Yang, X. (2016).
588 Emerging opportunities and challenges in phenology: a review. *Ecosphere, 7*(8).
589 Tateno, R., & Takeda, H. (2003). Forest structure and tree species distribution in relation to
590 topography-mediated heterogeneity of soil nitrogen and light at the forest floor.
591 *Ecological Research, 18*(5), 559-571.
592 Templ, B., Koch, E., Bolmgren, K., Ungersböck, M., Paul, A., Scheifinger, H., . . . Hodzić, S.
593 (2018). Pan European Phenological database (PEP725): a single point of access for
594 European data. *International Journal of Biometeorology, 62*(6), 1109-1113.
595 Vitasse, Y., & Basler, D. (2013). What role for photoperiod in the bud burst phenology of
596 European beech. *European Journal of Forest Research, 132*(1), 1-8.
597 Vitasse, Y., Signarbieux, C., & Fu, Y. H. (2018). Global warming leads to more uniform spring
598 phenology across elevations. *Proceedings of the National Academy of Sciences, 115*(5),
599 1004-1008.
600 Wareing, P. (1953). Growth studies in woody species V. Photoperiodism in dormant buds of
601 Fagus sylvatica L. *Physiologia Plantarum, 6*(4), 692-706.
602 Way, D. A., & Montgomery, R. A. (2015). Photoperiod constraints on tree phenology,
603 performance and migration in a warming world. *Plant, Cell & Environment, 38*(9), 1725-
604 1736.
605 Zohner, C. M., Benito, B. M., Svenning, J.-C., & Renner, S. S. (2016). Day length unlikely to
606 constrain climate-driven shifts in leaf-out times of northern woody plants. *Nature Climate*
607 *Change, 6*(12), 1120.
608 Zohner, C. M., & Renner, S. S. (2015). Perception of photoperiod in individual buds of mature
609 trees regulates leaf‐out. *New Phytologist, 208*(4), 1023-1030.
610

611 **Acknowledgments**

612 This work was supported by the NASA FINESST Program (80NSSC19K1356) and the College
613 of Liberal Arts and Science's (LAS) Dean's Emerging Faculty Leaders award at the Iowa State
614 University. ADR acknowledges support from NSF's Macrosystems Biology program (award EF-
615 1702697). JP acknowledges support from European Research Council grant ERC-SyG-2013-
616 610028. JM was supported by the Terrestrial Ecosystem Science Scientific Focus Area (TES
617 SFA) project funded by the US Department of Energy, Office of Science, Office of Biological
618 and Environmental Research. Oak Ridge National Laboratory is managed by UT-Battelle, LLC,
619 for the DOE under contract DE-AC05-1008 00OR22725. We acknowledge the E-OBS dataset
620 from the EU-FP6 project UERRA (http://www.uerra.eu) and the Copernicus Climate Change
621 Service, and the data providers in the ECA&D project (https://www.ecad.eu). We also
622 acknowledge all members of the PEP725 project for providing the phenological data.

623

624 **Data and materials availability**

625 All data needed to evaluate the conclusions in the paper are present in the paper and/or the
626 Supplementary Materials.

627

Figure Legends

Fig.1 Location of phenological observations for six species.

Fig.2 Latitudinal variations of elevation (a), temperatures (b), and daylength (c). Winter-spring temperature is the mean temperature from November 1st in the preceding year to April 30th. Winter temperature is the mean temperature from November 1st in the preceding year to January 31st and spring temperature is the mean temperature from February 1st to April 30th. Solid lines and shaded areas in (a) - (b) represent mean and variation (i.e., 25% and 75% quantiles) at 0.1° latitude bin, respectively.

Fig. 3 Changes in spring leaf-out across latitudes in the medium forcing group. Points and shaded areas represent mean and uncertainty (i.e., 50% of standard deviation), respectively, of spring leaf-out at a 0.1° latitude. We stratified the data into nine temperature groups based on three forcing and three chilling accumulations at high, medium, and low levels for each deciduous tree species based on the 33.3% and 66.6% quantiles of forcing or chilling accumulations during the period 1980-2016. Chilling is calculated as the number of days when daily mean temperature is below 5 °C from November 1st in the preceding year to leaf-out. Fitted linear regression lines for spring leaf-out with latitude are shown in each chilling group. Results for high and low forcing groups are shown in Figs. S3 and S4.

Fig.4 Evaluation of the photo-threshold (a), photo-chilling (b), and chilling-alone (c) models. Color of pixels represents the number of observations. The black 1:1 line, root mean square error (RMSE), and correlation (r) are shown.

Fig. 5 Observed and predicted slopes of spring leaf-out across latitudes for six deciduous tree species. The slopes (derived from the linear regressions in Fig. 6) represent the number of days changed in spring leaf-out per latitudinal degree increase. Positive slopes represent delayed spring leaf-out northward. Spring leaf-out data were selected from all site-year data during the period 1980-2016 based on the following two criteria: (1) forcing accumulation was within 65-75% quantiles of all forcing accumulations and (2) chilling accumulation was within 25-35% quantiles of all chilling accumulations. Significance is shown ($P < 0.01$).

Fig. 6 Observed (a) and predicted spring leaf-out by the photo-threshold model (b), photo-chilling model (c), and chilling-alone model (d) across latitudes. Color of pixels represents the number of observations. Spring leaf-out (day of year) were selected from all site-year data during the period 1980-2016 based on the following criteria: (1) forcing accumulation was within the 65-75% quantiles of all forcing accumulations and (2) chilling accumulation was within the 25-35% quantiles of all chilling accumulations. Gray lines represent the boundary of data distribution, fitted by a Loess smooth approach using the maximum and minimum spring leaf-out at each 0.1° latitude. Linear regression lines, slopes, and *P*-values for spring leaf-out against latitudes are shown. The results based on different selection criteria and sample sizes are shown in Figs. S6-S7.

Fig. 7 Interaction between photoperiod and temperature on spring leaf-out. Colors represent slopes (number of days changed in spring leaf-out per latitudinal degree increase) derived from Table 2 ($P < 0.01$). Positive slopes represent spring leaf-out was delayed northward. Gray indicates non-significant trend at $P > 0.05$. The color of the subfigures represents spring leaf-out (day of the year) with the same axes as the main figures. Spring leaf-out and the calculated forcing and chilling accumulation are from observation data.

Fig. 8 Model prediction of spring leaf-out and frost days during the period 2007-2100 for six deciduous tree species. Fitted linear regressions are shown for each model ($P < 0.001$). The subfigures are the accumulated frost days during the period 2007-2100. All three models predict no frost days for *F. excelsior* and *Q. robur*.

Table 1. Parameters and statistics of models calibration. Root mean square error (RMSE).

Models	**Photo-threshold model**				**Photo-chilling model**					**Chilling-alone model**			
Species	D^*_{start}	D^*_{end}	F^*	*RMSE*	*a*	*b*	*c*	T_{opt}	*RMSE*	*a*	*b*	T_{opt}	*RMSE*
Aesculus hippocastanum	10.7	15.5	90	9.92	518	-0.008	-0.12	-2.5	9.53	515	-0.0055	-3	12.04
Alnus glutinosa	10.7	15.5	86	14.30	500	-0.007	-0.01	-3.2	13.76	515	-0.0055	-3.2	15.87
Betula pendula	10.7	15.5	86	9.15	509	-0.008	-0.21	-3.2	8.92	515	-0.0055	-3.2	11.9
Fagus sylvatica	11.9	15.3	107	9.41	629	-0.011	-0.89	-3.2	8.81	579	-0.0055	-3	11.8

Fraxinus excelsior	11.7	15.5	176	9.95	630	-0.008	-0.9	-3.3	9.95	667	-0.0055	-3.2	11.66
Quercus robur	11.6	15.6	152	8.83	640	-0.008	-0.3	-3.3	8.82	635	-0.0055	-3.3	10.7

670 **Table 2. Slopes of spring leaf-out across latitudes in nine temperature groups.** Slopes represent the
671 number of days changed in spring leaf-out per latitudinal degree increase. Positive or negative slopes represent
672 delayed or advanced spring leaf-out northward, respectively. Forcing accumulation was defined as an
673 integration of daily mean temperature above 5 °C from November 1st in the preceding year to leaf-out. Chilling
674 was calculated as the number of days when daily mean temperature is below 5°C from November 1st in the
675 preceding year to leaf-out. Significant levels are shown as $P < 0.01$(***), $P < 0.05$(**), and $P < 0.1$(*).

Species	**Low forcing**			**Medium forcing**			**High forcing**		
Chilling	Low	Medium	High	Low	Medium	High	Low	Medium	High
Aesculus hippocastanum	0.882***	0.853***	0.145**	1.424***	0.443***	0.276***	0.891***	0.858***	-0.197**
Alnus glutinosa	0.414***	1.035***	0.035	1.445***	0.281***	0.211***	0.972***	0.542***	-0.268**
Betula pendula	0.998***	0.905***	-0.135**	1.629***	0.509***	0.291***	0.894***	1.029***	0.1
Fagus sylvatica	0.588***	0.676***	0.322***	1.209***	0.416***	0.17***	1.061***	1.118***	-0.122
Fraxinus excelsior	0.722***	0.62***	-0.015	1.611***	0.407***	0.13*	1.441***	0.912***	-0.286***
Quercus robur	0.769***	1.033***	0.473***	1.646***	0.574***	0.287***	1.353***	1.066***	-0.196**

676

677 **Table 3 Slopes of predicted spring leaf-out during 2007-2100 by three phenological models.** The slopes
678 are from fitted linear regression in Fig.8 ($P < 0.05$).

Slope	*Aesculus hippocastanum*	*Alnus glutinosa*	*Betula pendula*	*Fagus sylvatica*	*Fraxinus excelsior*	*Quercus robur*
Photo-threshold model	-1.86	-1.92	-1.87	-1.68	-1.80	-1.61
Photo-chilling model	-1.97	-2.00	-2.00	-1.63	-1.65	-1.64
Chilling-alone model	-4.12	-4.12	-4.12	-3.70	-3.15	-3.3

679

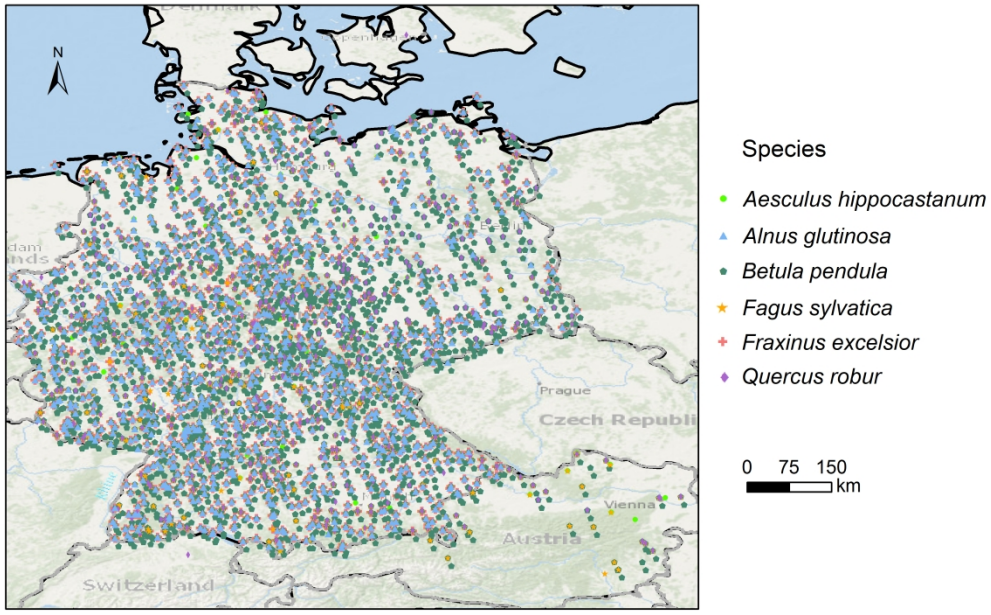

Fig.1 Location of phenological observations for six species.

244x153mm (400 x 400 DPI)

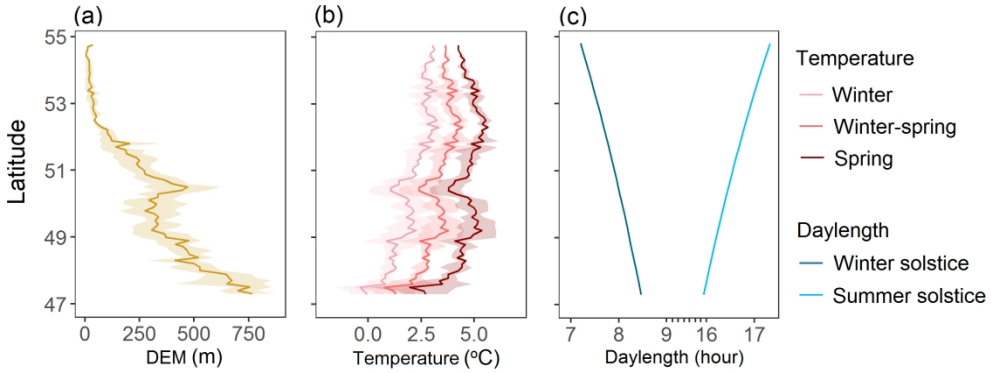

Fig.2 Latitudinal variations of elevation (a), temperatures (b), and daylength (c). Winter-spring temperature is the mean temperature from November 1st in the preceding year to April 30th. Winter temperature is the mean temperature from November 1st in the preceding year to January 31st and spring temperature is the mean temperature from February 1st to April 30th. Solid lines and shaded areas in (a) and (b) represent mean and variation (i.e., 25% and 75% quantiles) across all study sites at a 0.1o latitude, respectively.

209x78mm (300 x 300 DPI)

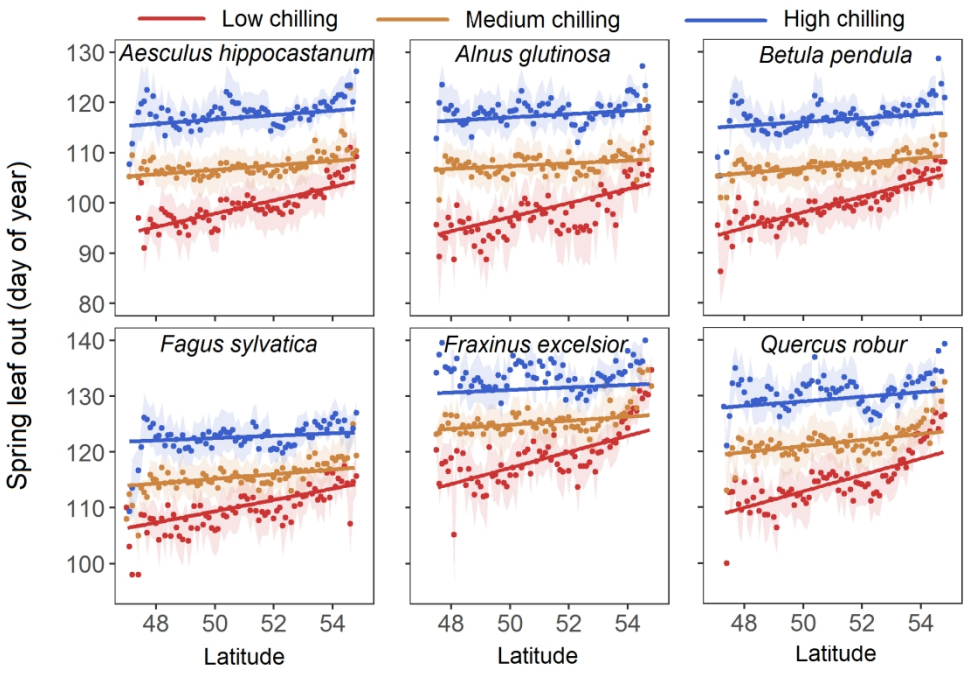

Fig. 3 Changes in spring leaf-out across latitudes in the medium forcing group. Points and shaded areas represent mean and uncertainty (i.e., 50% of standard deviation), respectively, of spring leaf-out at a 0.1o latitude. Chilling is calculated as the number of days when daily mean temperature is below 5 °C from November 1st in the preceding year to leaf-out. Fitted linear regression lines for spring leaf-out with latitude are shown in each chilling group. Results for high and low forcing groups are shown in Figs. S2 and S3.

370x251mm (144 x 144 DPI)

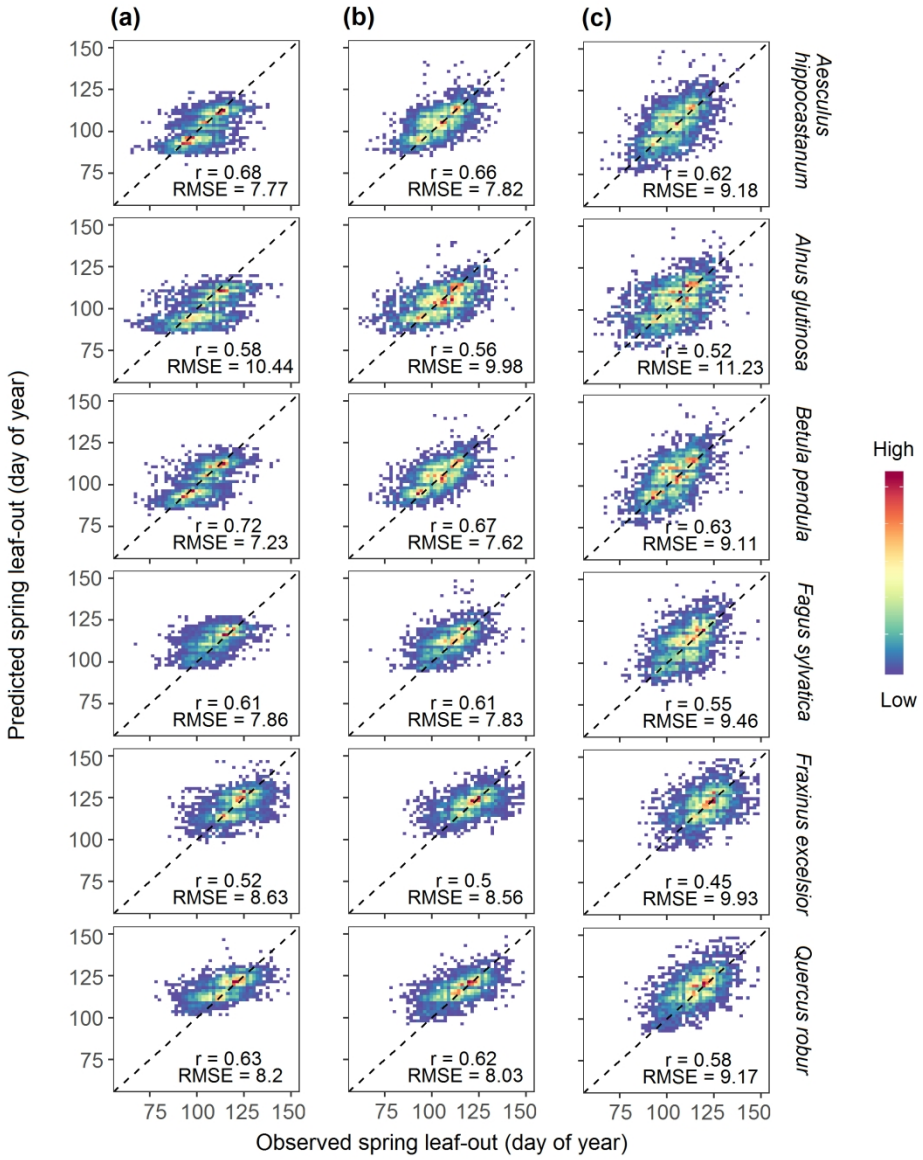

Fig.4 Evaluation of the photo-threshold (a), photo-chilling (b), and chilling-alone (c) models. Color of pixels represents the number of observations. The black 1:1 line, root mean square error (RMSE), and correlation (r) are shown.

419x488mm (144 x 144 DPI)

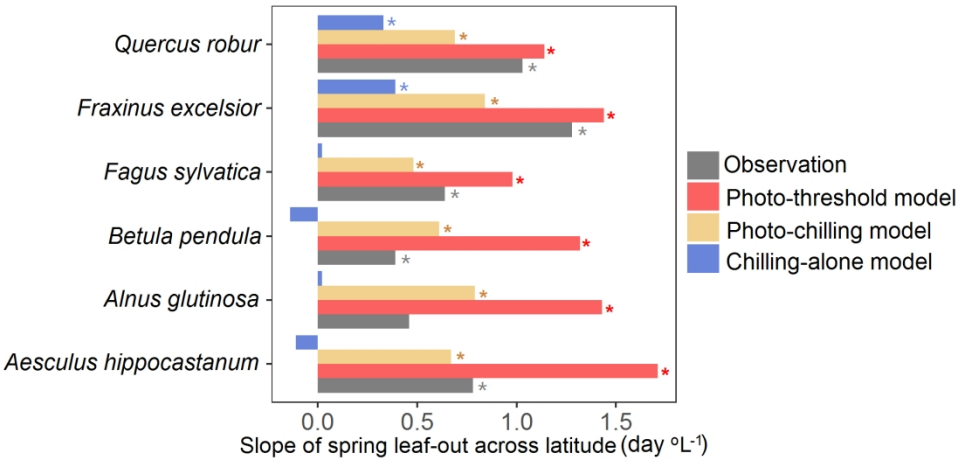

Fig. 5 Observed and predicted slopes of spring leaf-out across latitudes for six deciduous tree species. The slopes (derived from the linear regressions in Fig. 6) represent the number of days changed in spring leaf-out per latitudinal degree increase. Positive slopes represent delayed spring leaf-out northward. Spring leaf-out data were selected from all site-year data during the period 1980-2016 based on the following two criteria: (1) forcing accumulation was within 65-75% quantiles of all forcing accumulations and (2) chilling accumulation was within 25-35% quantiles of all chilling accumulations. Significance is shown ($P < 0.01$).

555x267mm (96 x 96 DPI)

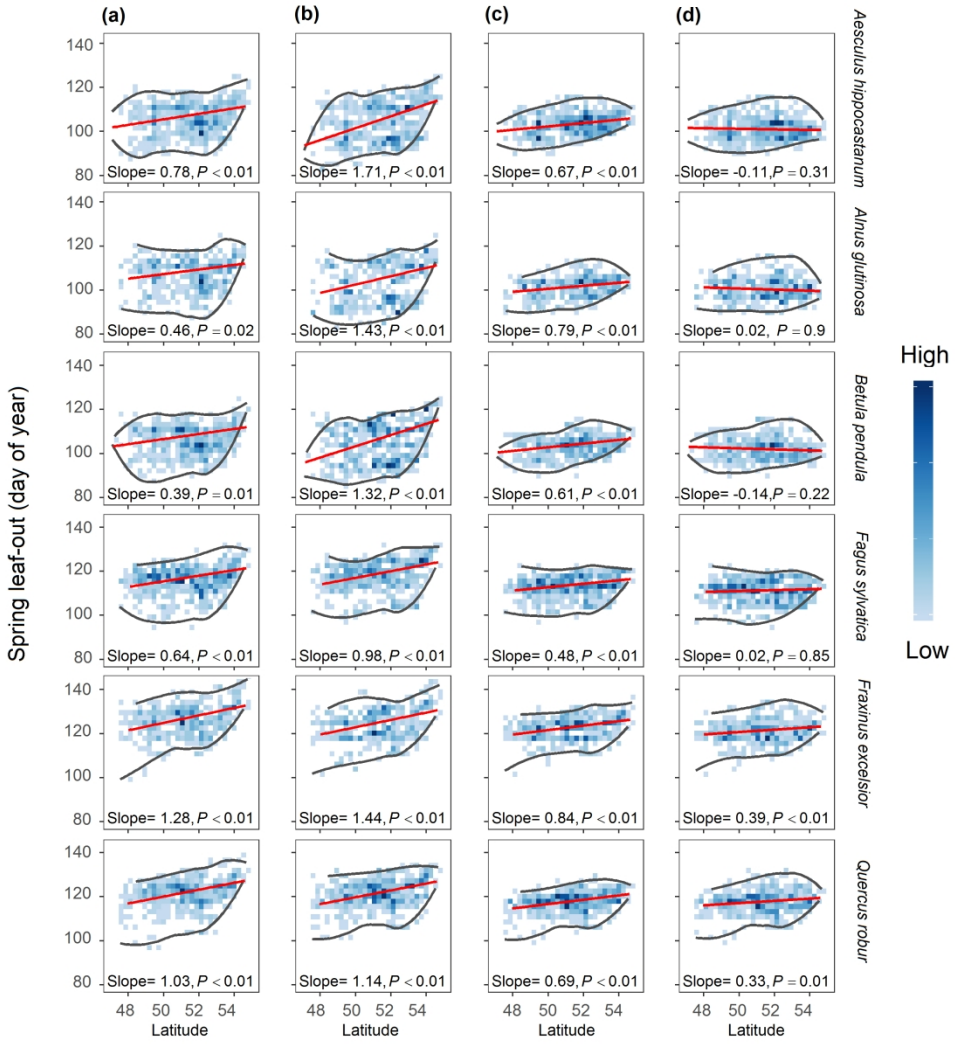

Fig. 6 Observed (a) and predicted spring leaf-out by the photo-threshold model (b), photo-chilling model (c), and chilling-alone model (d) across latitudes. Color of pixels represents the number of observations. Spring leaf-out (day of year) were selected from all site-year data during the period 1980-2016 based on the following criteria: (1) forcing accumulation was within the 65-75% quantiles of all forcing accumulations and (2) chilling accumulation was within the 25-35% quantiles of all chilling accumulations. Gray lines represent the boundary of data distribution, fitted by a Loess smooth approach using the maximum and minimum spring leaf-out at each 0.1o latitude. Linear regression lines, slopes, and P-values for spring leaf-out against latitudes are shown. The results based on different selection criteria and sample sizes are shown in Figs. S4-S5.

530x554mm (144 x 144 DPI)

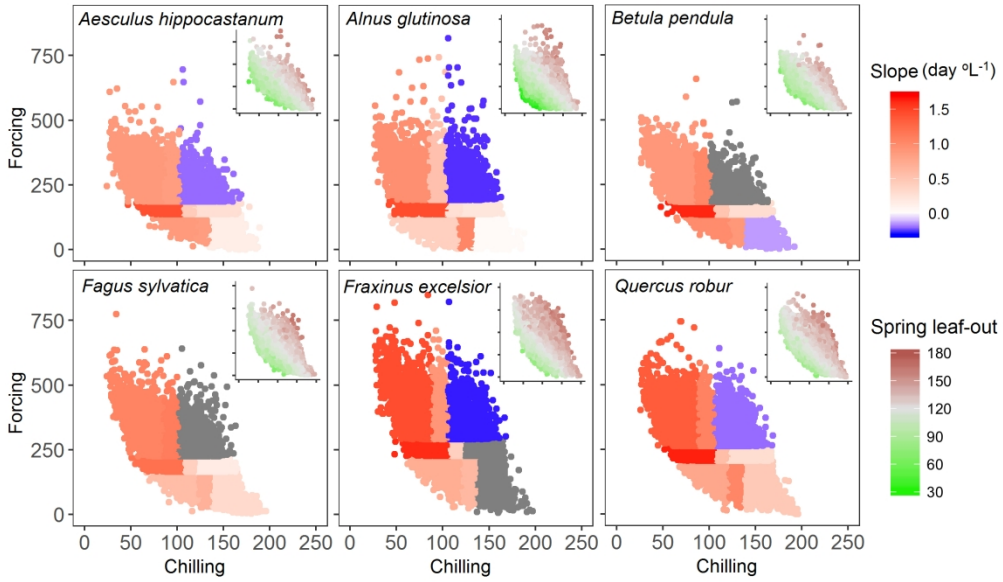

Fig. 7 Interaction between photoperiod and temperature on spring leaf-out. Colors represent slopes (number of days changed in spring leaf-out per latitudinal degree increase) derived from Table 2 ($P < 0.01$). Positive slopes represent spring leaf-out was delayed northward. Gray indicates non-significant trend at $P > 0.05$. The color of the subfigures represents spring leaf-out (day of the year) with the same axes as the main figures. Spring leaf-out and the calculated forcing and chilling accumulation are from observation data.

372x217mm (168 x 168 DPI)

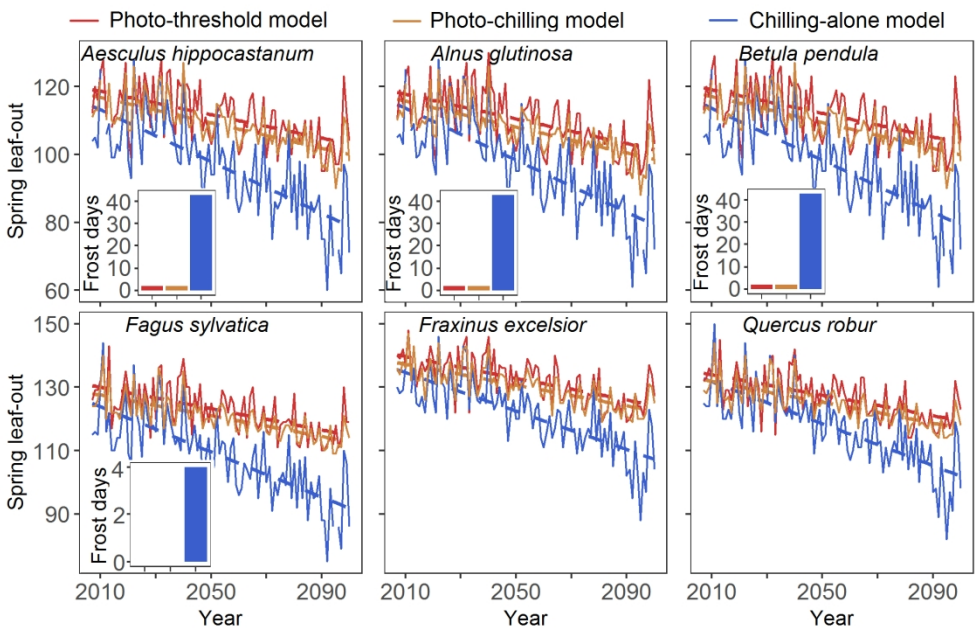

Fig. 8 Model prediction of spring leaf-out and frost days during the period 2007-2100 for six deciduous tree species. Fitted linear regressions are shown for each model ($P < 0.001$). The subfigures are the accumulated frost days during the period 2007-2100. All three models predict no frost days for F. excelsior and Q. robur.

391x250mm (144 x 144 DPI)